

# 3D SURFACE MICRO TOPOGRAPHY RECOVERY FROM MULTI-FOCUS IMAGES USING MODIFIED LAPLACIAN OPERATOR

Ji QI<sup>1</sup>, Yingzhong TIAN<sup>1\*</sup>, Wenjun ZHANG<sup>1</sup>, Albert WECKENMANN<sup>2</sup>, Minglun FANG<sup>1</sup>

<sup>1</sup> School of Mechatronic Engineering and Automation, Shanghai Key Laboratory of Intelligent Manufacturing and Robotics, Shanghai University, CHINA

<sup>2</sup> Chair Quality Management and Manufacturing Metrology, University Erlangen-Nuremberg, GERMANY, Albert.Weckenmann@qfm.uni-erlangen.de

\* Corresponding author: troytian@shu.edu.cn

## Abstract:

Optical microscopy enables the observation of highly magnified objects and material structures on micro surfaces, however with the weakness that it can only acquire 2D images. In order to observe the areal features more accurately and intuitively, 3D surface micro topography recovery is applied to form a 3D surface model of an object from its 2D image sequence. Optical microscope has a limited depth of focus in large magnification, which makes the area within the depth of focus cleared and other area blurred. So this paper firstly acquires image sequence which obtains all useful information in one view by vertical scanning of the microscope. Secondly, each image is calculated by an appropriate focus measure operator to find the maximum focus measure value and form a 2D fused image. Then the maximum value of each pixel is accurately transferred into a distance value, forming a discrete depth map. After conducting interpolation, fitting and color mapping, a smooth and authentic 3D color model of the measured surface is obtained. Various focus measure operators such as grey level variance are used to compare their performances in 3D model recovery. The superiority of the modified Laplacian operator proposed in this paper is proved by experimenting on measured objects with different micro topography features such as ditch shaped and slope shaped structure. In addition, surface roughness information of  $R_a$  and  $R_z$  is extracted from the formed 3D models.

**Keywords:** Modified Laplacian operator, micro topography, 3D surface recovery, focus measure, surface roughness

## 1. INTRODUCTION

Optical microscopy is a common and effective tool in laboratory for high-precision measurement, with function of enabling the observation of highly magnified objects and material structures on micro surfaces. However, it still has obvious disadvantages that it can only realize 2D measurement, not as comprehensive and intuitive as 3D measurement, and it has a limited depth of focus in large magnification, making the area within the depth of focus cleared and other area blurred, which is adverse to complete observation.

In order to solve the mentioned problems, the technology of 3D surface micro topography recovery is thus applied in this paper. Its process consists of two main stages: 2D image display and 3D model recovery. First of all, by vertical scanning of the objective lens on microscope, a multi-focus image sequence in which each image has a different clear area are captured by the CCD sensor. Then the former stage aims at processing on such an image sequence to form an all focused image with all areas clear, eliminating the visual

restriction caused by limited depth of focus. The method of this stage is also called image fusion technology based on time frequency[1]. The latter stage aims at forming an accurate 3D model after calculation of an appropriate focus measure operator on 2D image sequence, conducting fitting and interpolation on a depth map composed by discrete points, and finally mapping color information onto the model. The calculation of focus level on every pixel by choosing a proper mathematical operator is the core of this stage and also the research focus in this paper. Its theoretical basis is introduced as follows:

According to the convex lens model, shown in Fig. 1, if the sensing device where the image plane is on, is at a distance  $\delta$  from the focused plane, point P will be projected onto a blurred circle with radius R, being defocused. After decreasing the length of  $\delta$  until it is equal to zero, a best focused image can only be acquired at this time, when three variables of distance  $u$ , distance  $v$  and focal length  $f$  have a fixed relationship given by Gaussian lens law:  $1/f = 1/u + 1/v$ . Therefore, the finding of a maximum focus measure of every pixel from the image sequence, corresponding to this special location, is decisive in the stage of 3D model recovery. And this idea can also be seen in literature about shape from focus (SFF) and autofocus[2,3].

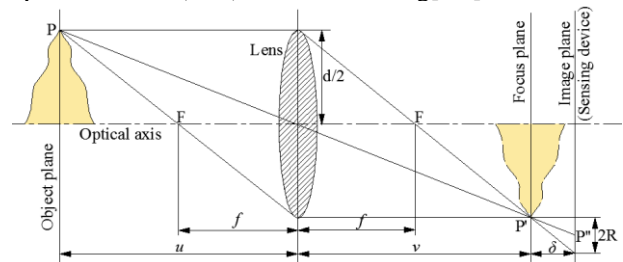


Fig. 1 Image formation principle in a convex model.  $d$ -aperture diameter,  $P$ -object,  $P'$ -focused point,  $P''$ -blurred circle,  $R$ -blurred circle radius,  $f$ -focal length,  $u$ -distance between object plane and lens,  $v$ -distance between focus plane and lens,  $\delta$ -distance between focus plane and image plane.

In the remainder of this paper, Section 2 describes the methodology of 3D surface micro topography recovery from different stages, and introduces the algorithms of the focus measure operators in detail. Section 3 describes the experiments and results to demonstrate the superiority of the proposed modified Laplacian operator performed in 3D model quality, both qualitatively and quantitatively. And the method of extracting surface roughness information from the 3D model is given. Section 4 concludes the whole paper.

## 2. METHODOLOGY

The methodology of 3D surface micro topography recovery consists of six stages: image acquisition, focus measure, 2D image display, 3D model recovery, result assessment and surface roughness measurement, among which the second one is the core of this paper and will be analyzed in detail.

### 2.1 Image acquisition

The step of image acquisition is the premise of the whole implementation procedure of measurement, using a hardware system which includes an optical metallurgical microscopy, a CCD camera, a computer, some accessories as well as some measured objects. The microscope is used to fix and observe the measured objects, obtaining the multi-focus image sequences by vertical scanning of the objective lens starting from an initial plane, shown in Fig. 2(a). Then the CCD camera acquires the images and delivers them to the computer as input for further process in software.

### 2.2 Focus measure

Focus measure is applied to measure the focus quality of every pixel in all images in the acquired sequence, which is a crucial step in the whole procedure and plays a decisive role in the precision of the generated 3D model.

By moving the sample in the vertical direction in relation to the objective lens, the degree of focus varies from low to high and back to low again. This change of focus is related to a change of contrast on the CCD sensor. By analyzing this contrast on the CCD sensor, the position where the sample is in focus can be measured[4]. As shown in Fig. 2(a), the central pixel in the 20<sup>th</sup> image has biggest contrast value with its neighborhood pixels among all 40 images in the sequence.

In order to measure the contrast, several popular algorithms or operators are applied here, one of which is called grey level variance (GLV). It comes from the principle that intuitively, high variance is associated with sharp image structure while low variance is associated with blurring, which reduces the amount of gray-level fluctuation[5]. The operator is shown as

$$FM_{GLV}(x, y) = \sum_{(i, j) \in W_{n \times n}} (I(x, y) - \mu)^2 \quad (1)$$

where  $W_{n \times n}$  is the local window with size of  $n \times n$  centered at  $(x, y)$ ,  $I(x, y)$  is the value of pixel  $(x, y)$ , and  $\mu$  is the mean value of  $W_{n \times n}$ .

Another type of the methods is based on derivatives. The Tenegrad focus measure (TEN)[3] is a gradient magnitude maximization method that measures the sum of the squared responses of the horizontal and vertical Sobel masks, shown in Eq. (2).

$$FM_{TEN}(x, y) = \sum_{(i, j) \in W_{n \times n}} (G_x(x, y)^2 + G_y(x, y)^2) \quad (2)$$

where  $G_x$  and  $G_y$  are the  $X$  and  $Y$  image gradients computed by convolving the given image  $I$  with the Sobel operators.

The Laplacian operator, being a point and symmetric operator, is suitable for accurate shape recovery. In order to solve the problem of zero Laplacian value and improve its robustness for weak-textured images, this operator is reformulated by Nayar and Nakagawa[6] to get a new equation, namely sum of the modified Laplacian (SLM) as

$$FM_{SLM}(x, y) = \sum_{(i, j) \in W_{n \times n}} \left( \left( \frac{\partial^2 g(x, y)}{\partial x^2} \right)^2 + \left( \frac{\partial^2 g(x, y)}{\partial y^2} \right)^2 \right) \quad (3)$$

In order to further simplify it, the discrete approximation to Eq.(3) is launched, and a variable spacing *step* to accommodate for possible variations in the size of texture elements is also added[6]. Hence, the equation is shown as

$$ML(x, y) = |2I(x, y) - I(x - step, y) - I(x + step, y)| \\ + |2I(x, y) - I(x, y - step) - I(x, y + step)| \quad (4)$$

$$FM_{SLM}(x, y) = \sum_{(i, j) \in W_{n \times n}} ML(x, y) \text{ for } ML(x, y) \geq T \quad (5)$$

where  $T$  is a threshold. The higher quality the input image sequence possesses, the shorter *step* is better to be used.

In this paper, Eq. (4) will be further improved by taking into consideration the influence from the neighbouring pixels of  $(x, y)$  along its diagonal direction. And thus a modified form of  $ML(x, y)$ , namely  $MML(x, y)$  is acquired, shown in Eq. (6). Experiment results show that this improvement will lead to a better effect of the 3D surface recovery.

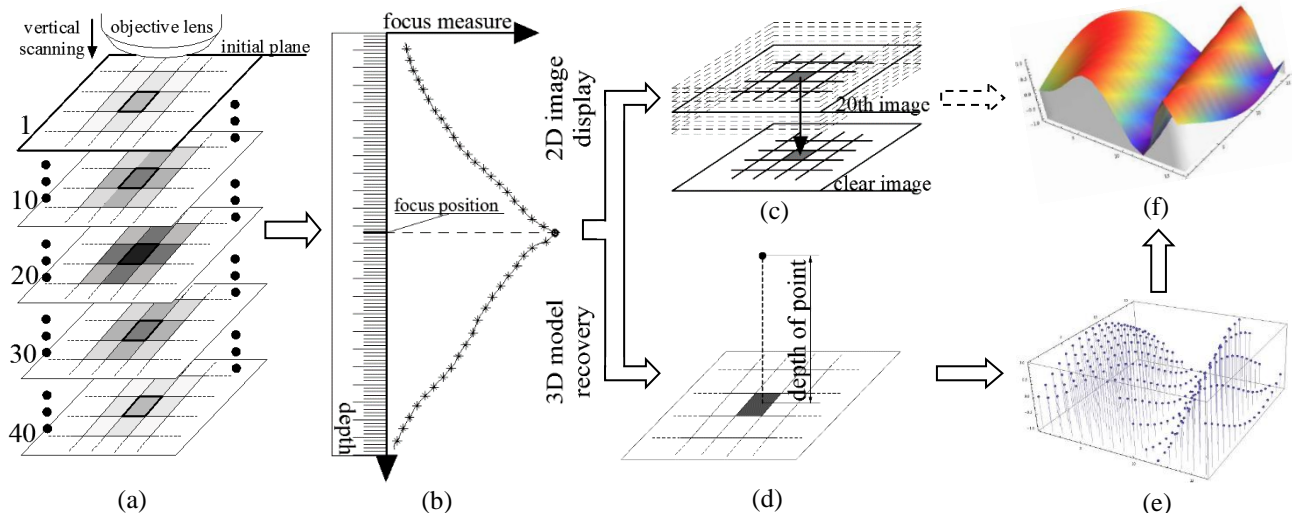


Fig. 2: Implementation procedure of 3D surface micro topography recovery. (a) Image acquisition, (b) Focus measure, (c) Formation of 2D fused image, (d) Calculation of depth of each point, (e) Discrete depth map, (f) 3D color model.

$$\begin{aligned}
 MML(x, y) &= |2I(x, y) - I(x - step, y) - I(x + step, y)| \\
 &\quad + |2I(x, y) - I(x, y - step) - I(x, y + step)| \\
 &+ |2I(x, y) - I(x + step, y - step) - I(x + step, y + step)| \\
 &+ |2I(x, y) - I(x - step, y - step) - I(x - step, y + step)| \quad (6) \\
 FM_{MSLM}(x, y) &= \sum_{(i,j) \in W_{msl}} MML(x, y) \text{ for } MML(x, y) \geq T \quad (7)
 \end{aligned}$$

For each pixel, the value of  $FM$  is not equal to the real depth value, hence a depth calculation function  $D(x, y)$  is figured out as Eq. (7) by depth calibration and precise calculation, which builds a relationship between maximum value of  $FM$  and real depth value.

$$d(x, y) = DF(\max(FM(x, y))) \quad (8)$$

After the calculation of each operator, a collection of focus measure values are thus acquired. To make the discrete points continuous, Gaussian interpolation is adopted to model the focus measure function  $F(d)$  and interpolates the computed measure values to obtain more accurate depth estimates, resulting in a function curve as shown in Fig. 2(b). Considering only the maximum value is needed and the purpose of saving computations, the algorithm only uses three values, namely,  $F_{m-1}$ ,  $F_m$  and  $F_{m+1}$ , that lie on the largest mode of  $F(d)$ , such that  $F_m > F_{m-1}$  and  $F_m > F_{m+1}$ . Shown as Fig. 3, then the maximum value  $F_{peak}$  is obtained, and its corresponding depth value  $\bar{d}$  is figured out, which will be used in the following step of depth map generation.

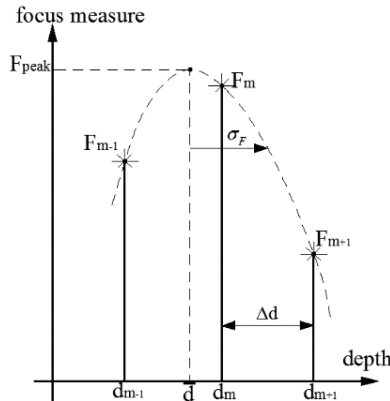


Fig. 3: Gaussian interpolation of focus measures.

### 2.3 2D image display

In the step of 2D image display, a fused 2D image with all areas clear in the scene can be obtained, solving the drawback that in the source images, the areas within the depth of focus cleared and other areas blurred caused by limited depth of focus in large magnification. Thus the fused image is more suitable for human visual perception and meets the requirements of 2D image measurement. The implementation procedure is firstly to create a 2D empty matrix having the same size as the source images, then map each one of the pixels which exhibits the highest focus measure value from its corresponding image to the empty matrix at the same position. For example, the pixel at  $(x, y)$  from the 20<sup>th</sup> image is mapped to the empty matrix. Hence a clear and fused image is generated, shown in Fig. 2(c) and this method can also be found in Ref.[1], in which it's called image fusion algorithms based on time domain.

### 2.4 3D model recovery

A 3D color model can precisely reflect position, height and color information of the microscopic surface of the measured object. The whole implementation procedure of 3D model recovery, shown in Fig. 2(d),(e)&(f), mainly includes three steps as below:

- (1) After all depth values for every pixel are calculated, the collection of the depth values will generate a 3D depth map.
- (2) Cubic spline interpolation method is applied on the depth map to make the 3D model continuous and smooth, closer to the real surface micro topography.
- (3) The color value of each pixel in the 2D fused image is directly mapped to the corresponding position on the 3D model in step (2).

### 2.5 Result assessment

After obtaining 3D models by different kinds of focus measure operators, it's necessary to use some Image Quality Assessment (IQA) indicators to conduct quantitative analysis. For the reason that 2D image display and 3D model recovery are both based on a matrix of focus measure values mentioned in the stage of 'focus measure', the qualities of the fused image and 3D model are directly linked. So in this stage, only the 2D image results are assessed by two IQA indicators to test their qualities. Malik and Choi[7] and Mahmood et al.[8] used root mean square error (RMSE) as an indicator. The smaller RMSE an image has, the better quality it has. Lee et al.[3] used peak signal-to-noise ratio (PSNR), and a bigger PSNR means better quality of the result.

### 2.6 Surface roughness measurement

Surface roughness information of an area on the measured object can be extracted from a certain contour on this area, shown as Fig. 4(a). There are two common evaluation parameters for surface roughness:

- (1) Arithmetic mean deviation of the assessed contour  $R_a$ , which is the arithmetic mean of integral of absolute deviated distance  $I(x)$  within a sampling length  $l$  on the contour of measured object. Formula of this parameter is shown as Eq. (9) and Fig. 4(b):

$$R_a = \frac{1}{l} \int_0^l |I(x)| dx \quad (9)$$

- (2) Maximum height of the assessed contour  $R_z$ , which is the sum from the height of the highest contour peak and the depth of the lowest contour valley within a sampling length  $l$ . Formula of this parameter is shown as Eq. (10) and Fig. 4(b):

$$R_z = I(x)_{p \max} + I(x)_{v \max} \quad (10)$$

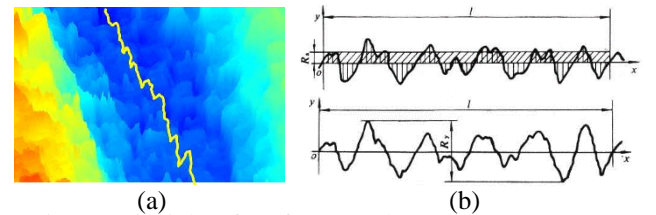


Fig. 4: Principle of surface roughness measurement. (a) Surface contour of 3D model (yellow), (b) Calculation method of  $R_a$  and  $R_z$ .

### 3. EXPERIMENTS AND RESULTS

In this section, a group of 3D surface micro topography recovery experiments are conducted, using a hardware system composed by a metallurgical microscope, a CCD sensor and a computer, as well as a software tool of Matlab. And the measured objects are a series of precision reference specimens produced by Rubert & Co Ltd., England, which have surfaces that have been carefully worked by shaping, end-milling, grinding and other processes.

#### 3.1 Comparative experiments

In order to compare performance of different operators, a distinctive ditch shaped surface topography is selected for model recovery, captured in an image sequence consisting of 26 images of 768X432 pixels, with acquisition step of every one micrometer. Fig. 4 shows all the results of  $FM_{GLV}$ ,  $FM_{TEN}$ ,  $FM_{SML}$ , and  $FM_{MSML}$  with four window sizes respectively. The rainbow colored models are smooth and continuous models after conducting cubic spline interpolation on discrete depth maps. Color varies from red to blue, along with the variation from low depth to high depth, and thus depth information of the 3D model can be judged from the colors of each point. The fewer noises are on a model, namely points with extremely higher values than their neighbouring ones, the better quality a model owns. Fig. 4 (fifth column) shows color models after color mapping and Fig. 4 (sixth column) shows 2D fused images.

#### a) Comparison on performance of focus measure operators

From Fig. 4 and Table 1, some conclusions can be achieved by qualitative and quantitative analysis.

It's evident that  $FM_{GLV}$  has worst effect among all focus measure operators for its numerous noises on models, proved by biggest RMSE and smallest PSNR in Table 1.

Models of  $FM_{TEN}$  have much fewer noises than  $FM_{GLV}$ , and when window size increases to 17X17, both indicators are improved. Models of  $FM_{SML}$  with different window size have very few noises, bringing satisfactory performance. By contrast, Models of  $FM_{MSML}$  also have very few noises, especially when window size is 17X17. After conducting quantitative analysis, its smallest RMSE and biggest PSNR prove that it has better performance than  $FM_{SML}$  and it is the best one among all operators. Hence  $FM_{MSML}$  is advised in measurements using 3D model recovery technology.

Table 1: Results of IQA indicators on fused images

	$FM_{GLV}$	$FM_{TEN}$	$FM_{SML}$	$FM_{MSML}$
RMSE	0.0303	0.0299	0.0262	0.0258
PSNR	30.3680	30.4753	31.6205	31.7812

#### b) Selection of window size

The increasing of window size results in decreasing of noises on models, which means high accuracy of the results. However, the increasing of window size will meanwhile increase computation amount and reduce the quality of results by excessively smoothing the model surface[9]. Fig. 4 shows that models with window size of 17X17 have best performance, and according to the experimental results, if the window size exceeds 17X17, the quality of models will not be obviously improved. On the other side, the time consumption of calculation will substantially increase, shown in Table 2, which is adverse to the rapid realization of algorithms. In conclusion, window size around 17X17 is suggested in 3D model recovery.

Table 2: Time consumption of  $FM_{MSML}$  with different window size

	5X5	9X9	13x13	17X17	21X21	25x25	29X29
Time (s)	40	50	75	110	160	220	300

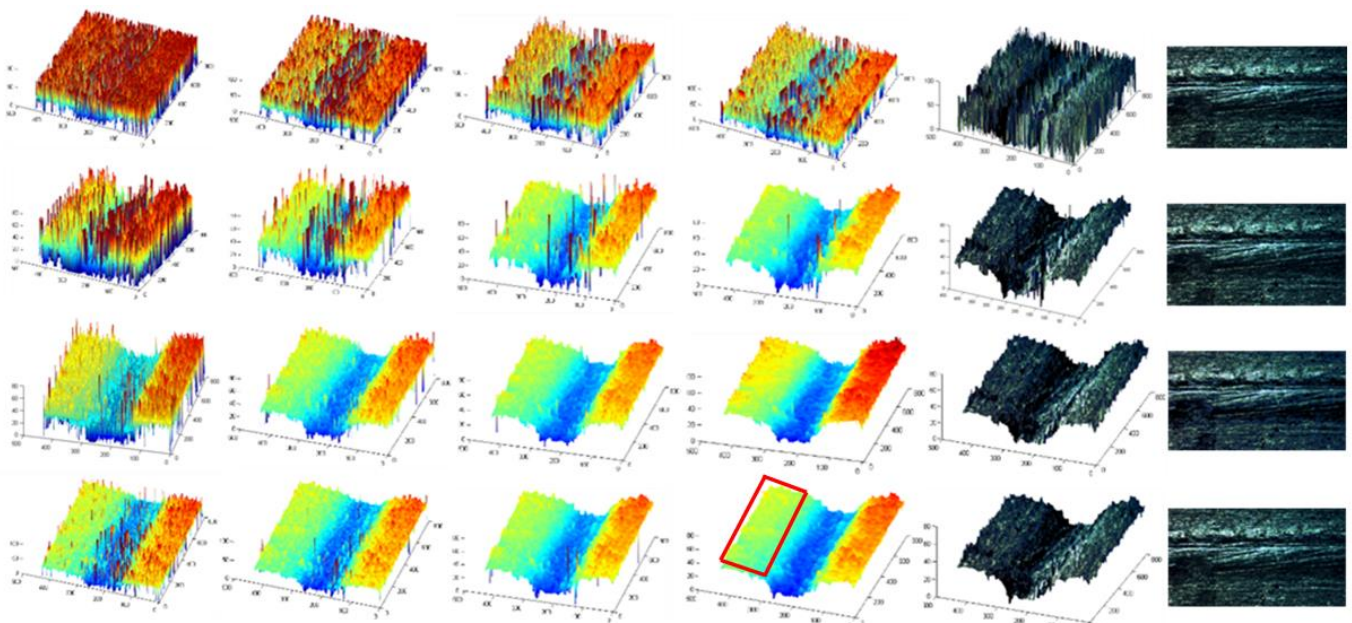


Fig. 4: 3D models of precision reference specimen of shaping:  $FM_{GLV}$ (first row),  $FM_{TEN}$ (second row),  $FM_{SML}$ (third row),  $FM_{MSML}$ (fourth row); window size of 5X5 (first column), 9X9 (second column), 13X13 (third column), 17X17 (fourth column); models after color mapping with window size of 17X17 (fifth column); 2D fused images with window size of 17X17 (sixth column).

### 3.2 Verification experiments

In order to verify the correctness of conclusions summarized in comparative experiments, a set of verification experiments using  $FM_{MSML}$  and window size of 17X17 are conducted. Fig. 5 (first column) shows the results of a reference specimen of grinding, featured by smooth surface and slope shape. And Fig. 5 (second column) shows the results of a reference specimen of end-milling, featured by uneven surface and convex shape. These two sets of experiments both result in few noises and high quality, which means the proposed method can adapt to micro topography with different features. Additionally, Fig. 5 (third column) has the same scene as Fig.4 (sixth column), but the former one is captured under bright field, resulting that it has worse quality and more information loss than the later one. This reflects that the quality of 3D model is directly related to the quality of its source images.

### 4. CONCLUSIONS

In this paper, a complete procedure of realizing 2D image fusion and 3D color model recovery is given. In this procedure, focus measure is the core step and the performance of focus measure operator has significant influence on the quality of 3D model. So this paper proposes a modified Laplacian operator MSML and experiments on four operators: GLV, TEN, SML and MSML to demonstrate that MSML with window size of 17X17 can bring the best effect. Verification experiments conducted on objects with various micro topography features proves the correctness of the conclusions. Finally, surface roughness parameters  $R_a$  and  $R_z$  are measured on the 3D model, which has important research significance and practical values.

### REFERENCES

- [1] A.A. Goshtasby, S. Nikolov. "Image fusion: advances in the state of the art", *Information Fusion*, vol.8, pp. 114-118, 2007.
- [2] Rashid Minhas, et al., "Shape from focus using fast discrete curvelet transform", *Pattern Recognition*, vol.44, pp. 839-853. 2011.
- [3] Ikhyun Lee, et al., "Adaptive window selection for 3D shape recovery from image focus", *Optics & Laser Technology*, vol.45, pp. 21-31, 2013.
- [4] R. Leach, "Optical Measurement of Surface Topography", *Springer*, pp. 131-166, 2011.
- [5] Yeo T, Ong S, et al., "Autofocusing for tissue microscopy", *Image and Vision Computing*, vol.11, pp. 629-639, 1993.
- [6] Nayar S. and Nakagawa Y., "Shape from focus", *IEEE Transactions on Pattern Analysis and Machine Intelligence*, pp. 824-831, 1994.
- [7] A.S. Malik, T.S. Choi, "A novel algorithm for estimation of depth map using image focus for 3D shape recovery in the presence of noise", *Pattern Recognition*, vol.41, pp. 2200-2225. 2008.
- [8] M.T. Mahmood, et al., "Shape from focus using principal component analysis in discrete wavelet transform", *Optical Engineering*, vol.48. 2009.
- [9] Said Pertuz, et al., "Analysis of focus measure operators for shape-from-focus", *Pattern Recognition*, vol.46, pp. 1415-1432, 2013.

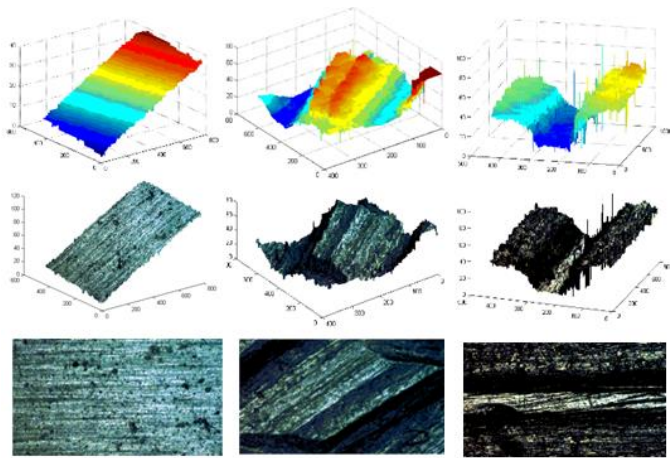


Fig. 5: 3D colorless models (first row), color models (second row), and 2D fused images (third row) of reference specimens of grinding (first column), end-milling (second column) and shaping (third column), with all using  $FM_{MSML}$  and window size of 17X17.

### 3.3 Calculation of surface roughness

Fig. 6(a) is the top view of a generated model and the contour along the red line is measure, shown in Fig. 6(b). According to Eq. (9)&(10), after calculation, the roughness parameter  $R_a$  is 1.785 $\mu\text{m}$  and  $R_z$  is 10.415 $\mu\text{m}$ , both marked in Fig. 6(c).

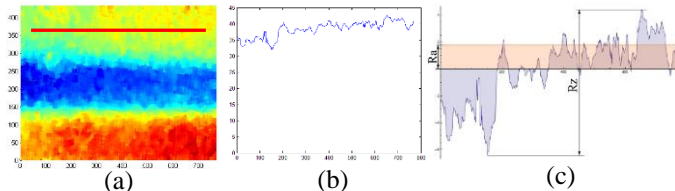


Fig. 6: Calculation of surface roughness. (a) Top view of the model using  $FM_{MSML}$  and window size of 17X17, (b) Surface contour along the red line in (a), (c)  $R_a$  and  $R_z$  along the red line.

